Applied Surface Science 257 (2011) 6112–6117

Contents lists available at ScienceDirect

Applied Surface Science

journal homepage: www.elsevier.com/locate/apsusc

New optical features to enhance solar cell performance based on porous silicon surfaces

Asmiet Ramizy[a,*], Z. Hassan[a], Khalid Omar[a], Y. Al-Douri[b,*], M.A. Mahdi[a]

[a] Nano-Optoelectronics Research and Technology Laboratory, School of Physics, Universiti Sains Malaysia, 11800 USM, Penang, Malaysia
[b] Institute of Nano Electronic Engineering, University Malaysia Perlis, 01000 Kangar, Perlis, Malaysia

ARTICLE INFO

Article history:
Received 18 November 2010
Received in revised form 30 January 2011
Accepted 4 February 2011
Available online 5 March 2011

PACS:
61.43.Gt
88.40.H–
72.80.Jc
78.20.Ci

Keywords:
Porous silicon
Solar cell
Crystalline silicon
Refractive index

ABSTRACT

Electrochemical etching is used to fabricate porous silicon (PS) surfaces for both sides of the Si wafer. The effect of PS on performance of Si solar cells is investigated and the reflected mirrors are manipulated to enhance solar cell efficiency. The process is promising for solar cell manufacturing due to its simplicity, lower cost and suitability for mass production. The PS surface has discrete pores and short-branched pores on the polished wafer side. In contrast, the etched backside of the wafer has smaller pore size, with random pores. PS formed on both sides has lower reflectivity value compared with results in other works. Solar cell efficiency is increased to 15.4% with PS formed on both sides compared with the unetched sample and other results. Using empirical models, the optical properties of the refractive index and the optical dielectric constant are investigated. The porous surface texturing properties could enhance and increase the conversion efficiency of porous Si solar cells. The obtained results are in agreement with experimental and other data.

1. Introduction

The amount of reflection from a surface is the main obstacle in efficient solar cell performance. Reflection is related to the refractive index of the material. For instance, the silicon (Si) refractive index is 3.5 (which can rise by up to ~35%) which prevents an electron–hole pair from being generated. This factor could reduce the efficiency of photovoltaic converters. Antireflection Coatings (ARC) could reduce surface reflection, and increase conversion efficiency, extended lifetime and improved the electro-physical and characterization of photovoltaic converters [1].

Porous Si (PS) is attractive in solar cell applications due to its efficient ARC and other properties such as band gap broadening, wide absorption spectrum and optical transmission range (700–1000 nm). It can also be used for surface passivation and texturization [2–6]. The potential advantages of PS as an ARC for solar cells include surface passivation and removal of the dead layer diffused region. Moreover, PS could convert higher energy solar radiation into spectrum light, which is absorbed more efficiently into bulk Si [7].

The vibrations, electronic and optical properties of PS have been studied using various experimental techniques. Of these, the electrochemical etching process is a promising technique in fabricating PS [8–11]. According to the quantum confinement model, a heterojunction can be formed between the Si substrate and porous layers because the latter has a wider band gap (1.8–2.2 eV) compared with crystalline Si (c-Si) [12].

Recently, Ben Rabha and Bessais [13] used Chemical Vapor Etching (CVE) method to perform front PS layer and Buried Metallic Contacts (BMCs) of multicrystalline Silicon (mc-Si) solar cells to reduce the reflectivity to 8% in the 450–950 nm wavelength range and induced the simple and low cost technology with 12% conversion efficiency. Yae et al. [14] have deposited fine platinum (Pt) particles on multicrystalline *n*-Si wafers by electroless displacement reaction in a hexachloroplatinic acid solution containing HF. The reflectance of the wafers is reduced from 30% to 6% by the formation of porous layer. Brendel [15] has performed electrochemical etching of porous Si layer into the substrate based on homoepitaxial growth of monocrystalline Si films and yielded a module efficiency of 10%.

This work aims to investigate the effect of PS on performance of Si solar cells. Enhancing solar cell efficiency can be realized by manipulating reflected mirrors. The results are promising for solar cell manufacturing, as they show the simplicity, lower cost, suitability for mass production and to investigate

* Corresponding authors.
E-mail addresses: asmat_hadithi@yahoo.com (A. Ramizy), yaldouri@yahoo.com (Y. Al-Douri).

0169-4332/$ – see front matter © 2011 Elsevier B.V. All rights reserved.
doi:10.1016/j.apsusc.2011.02.013

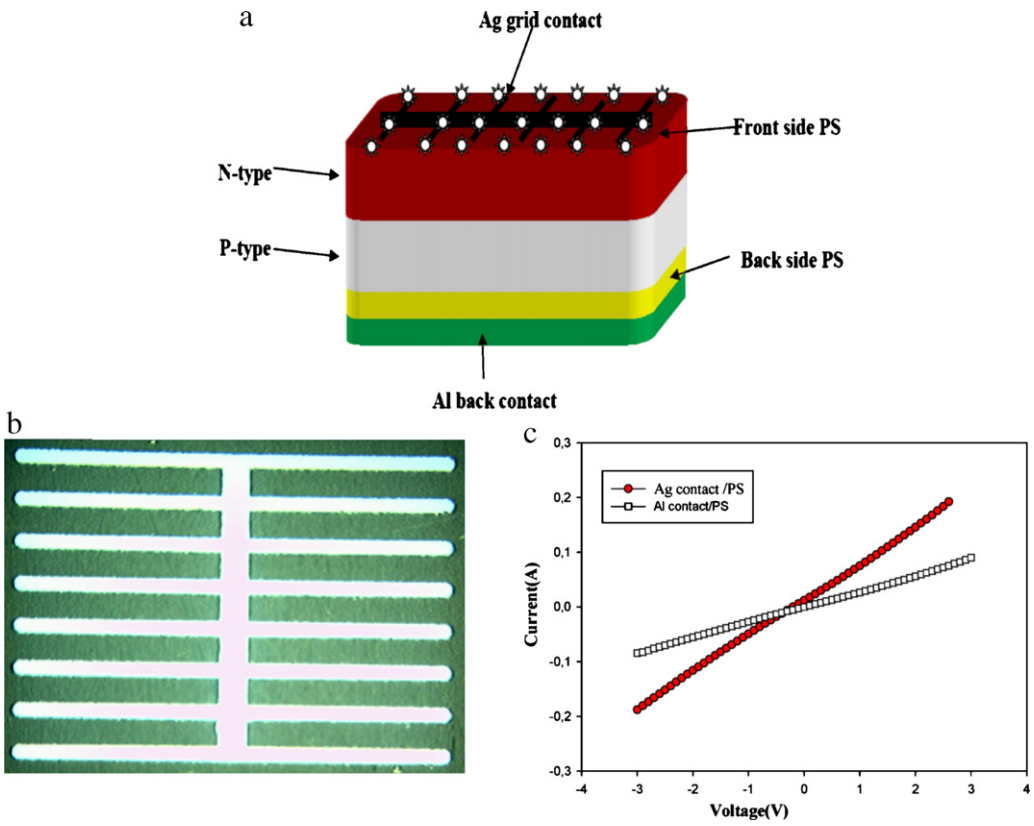

Fig. 1. Solar cells setup (a) p–n junction layers, (b) metal mask, and (c) contact *I–V* characterization.

the optical properties of refractive index and optical dielectric constant.

This paper is arranged as follows. Section 2 discusses the experimental procedure, while the experimental and theoretical results are in Section 3. The conclusion is provided in the last section.

2. Experimental measurement

N-type Si wafer with a dimension of 1 cm × 1 cm × 283 μm, (1 1 1) orientation, resistivity of 0.75 Ω cm, and doping concentration of 1.8×10^{17} cm^{-3} was etched through an electrochemical process to produce the porous structure. The wafer was placed in an electrolyte solution (hydrofluoric (HF) acid: ethanol, 1:4) with a current density of 60 mA/cm^2 at an etching time of 15 min for each side. Before the etching process, the Si substrate was cleaned using the Radio Corporation of America (RCA) method to remove the oxide layer, it was then immersed in HF acid to remove the native oxide. The electrochemical cell was made by teflon and has a circular aperture with radius of 0.4 cm, and the silicon wafer is sealed below. The cell consists of two-electrode system with the Si wafer as the anode and platinum as the cathode. The process was carried out at room temperature. After etching, all samples were rinsed with ethanol and dried in the air. Surface morphology and structural properties of the samples under treatment were characterized by using Scanning Electron Microscopy (SEM). PS optical reflectance was obtained by using an optical reflectometer (Filmetrics F20) that includes integrating sphere. Fourier Transform Infrared Spectroscopy (FTIR) of the PS samples was measured. Photoluminescence (PL) spectroscopy measurements were performed at room temperature using He–Cd laser (λ = 325 nm).

To fabricate the solar cell; After (RCA) cleaning and oxidation, the silicon wafer underwent spin coating. A liquid containing photo-resistant material was placed at the center of the wafer. Spinning process was carried out at room temperature at the speed of 300 rpm for 20 s. After spin coating, the wafer was placed back into the furnace for 20 min at 200 °C to drive out moisture. The mask was designed by the photo plotter technique that was placed directly above the sample and exposed to UV-light for 25 s to form a patterned coating on the surface. Doping diffusion was carried out using a tube furnace at the temperature of 1100 °C for 60 min using N2 flow gas. The top surface area of the wafer was doped with boron to be P-type. Prior to the contact evaporating process, the oxidation layer was removed using an etching solution of NH_4F:H_2O, and then mixed with HF with a mole ratio of 1:7. Aluminum evaporation was used for back metal contact, and silver was used for front metallization. Fig. 1 shows solar cells setup. Contact annealing was done at 400 °C for 20 min to pledge ohmic contact (see Fig. 1) as well as to improve the contact properties. Reflected mirror with reflectivity >89% was used to enhance solar cell efficiency. The structure of PS solar cells consists of metal mask contact of grid pattern with finger width of 300 μm, and finger spacing of 600 μm.

The fabricated device was analyzed using current–voltage (*I–V*) measurement, and the lens was placed under solar simulator illumination. A solar cell using unetched c-Si was fabricated under the same conditions for comparison.

3. Results and discussion

The efficiency of photovoltaic energy conversion must be enhanced to reduce the cost of solar cell modules for energy generation. In this process, photons from solar radiation are falling on a solar cell generate electron and hole pairs, which are collected at the two contact points. A drawback of solar photovoltaic energy con-

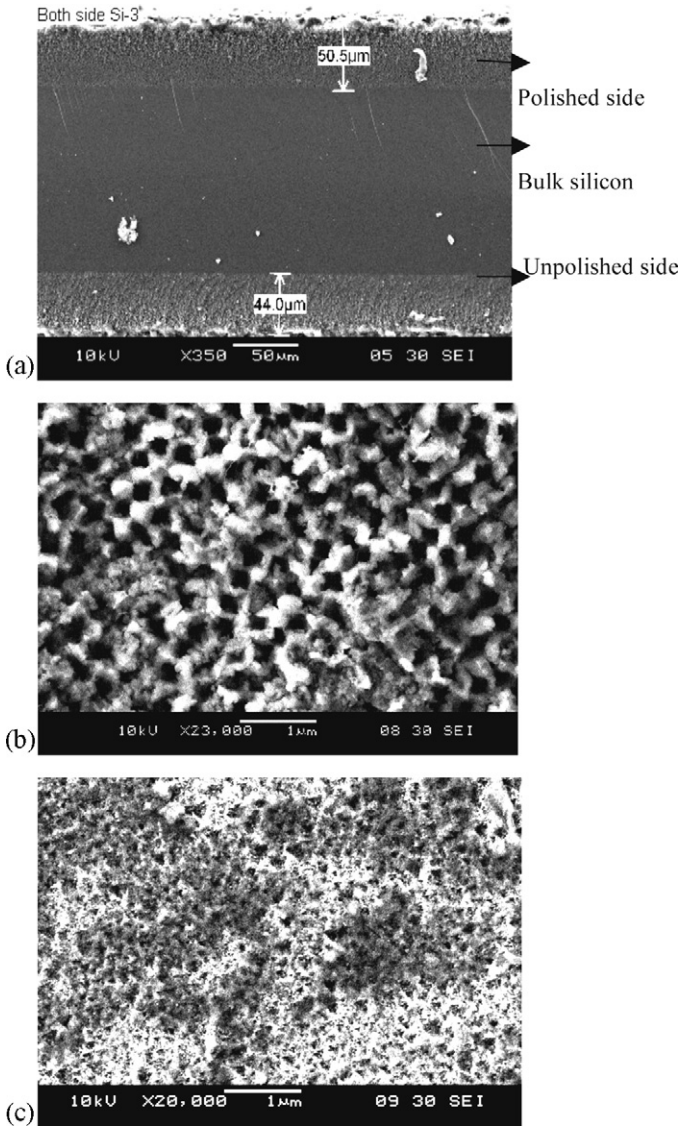

Fig. 2. Cross-section SEM images of PS on (a) both sides of the c-Si wafer, (b) on the polished front side c-Si wafer and (c) on the unpolished backside c-Si wafer.

version is that most semiconducting materials used are sensitive to only a part of the solar radiation spectrum.

Fig. 2a shows the cross-section SEM images of chemically treated samples. These images show that the thickness is uniform throughout the obtained porous layer, indicating that the etching process forms a uniform porous density layer on the surface. The SEM images in Fig. 2b and c illustrate the treated surface with similar grain geometry due to the isotropic character of HF/ethanol etching and the optimal conditions of current density and etching time. The images show that the entire surface of the sample was etched. Most pores are spherical. The porous surface formed on the front polished side had discrete pores, in addition to short-branched pores. In contrast, the PS surface formed on the unpolished backside is shaped in small pores, which could be attributed to an increase in surface roughness for the unpolished backside proportional to the etching parameter. Fig. 3 demonstrates that the three dimensional topographic images of the PS etched surfaces with the pyramidal shape were distributed over the entire surface. The pyramidal shape indicated that the increase in the surface roughness is due to the effect of the etching parameters' effect on the surface characterization. The high degree of roughness

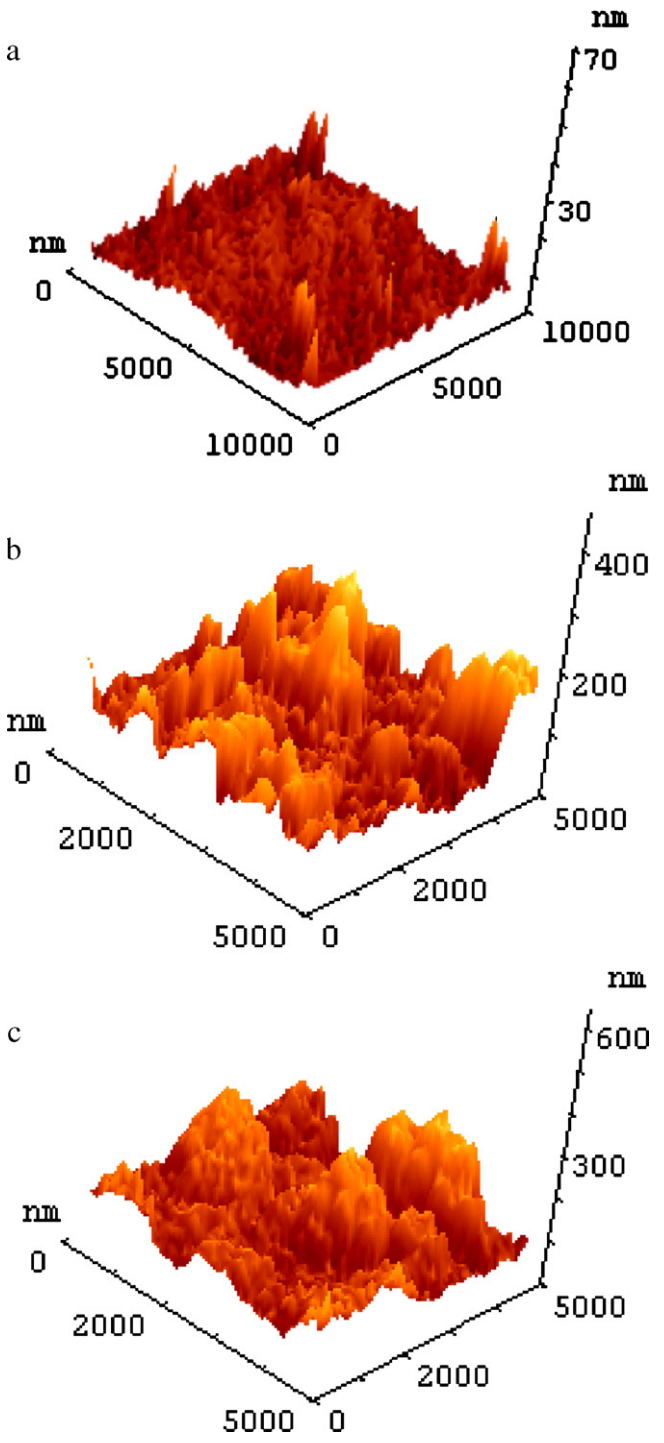

Fig. 3. AFM images of PS (a) as-grown, (b) polished front side and (c) unpolished back side.

of the PS surface implies the possibility of using the porous layer as an ARC because the surface texture reduces the light reflection. The scattering in PS is possibly due to the roughness in relation to the thickness of the porous layer [16]. The attenuation of the reflectivity is due to scattering and transmission at the porous and bulk interfaces [16,17]. This parameter is important in enhancing the photo conversion process for solar cells. To confirm that PS can be utilized as an ARC, the reflection measurement was done by using optical reflectometry.

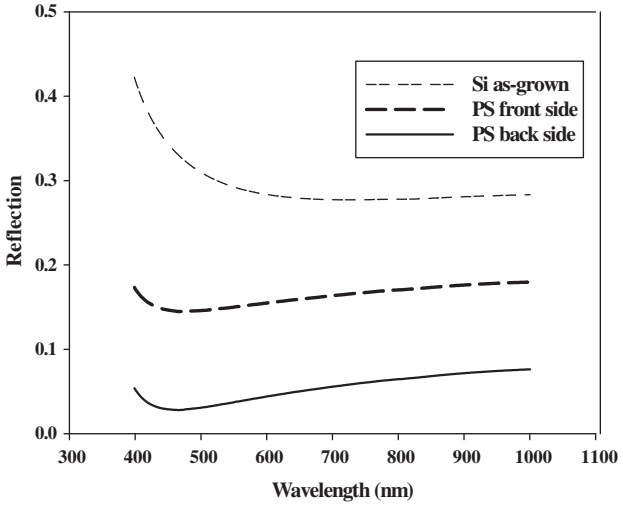

Fig. 4. The reflectance spectra of Si (as grown) and PS of both sides.

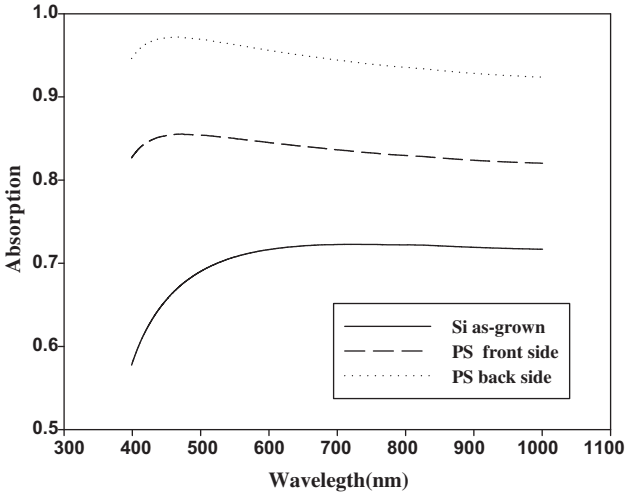

Fig. 5. The absorption spectra of Si (as grown) and PS of both sides.

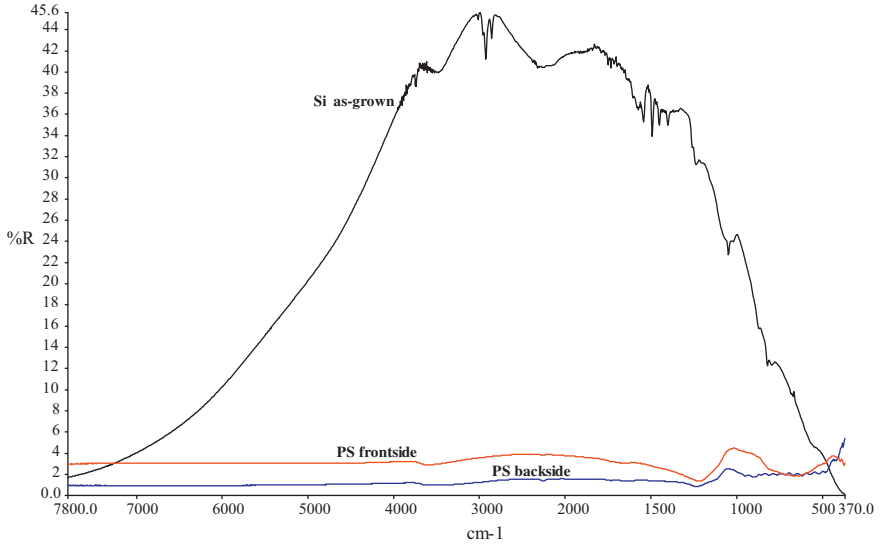

Fig. 6. FTIR reflection spectra of Si (as grown) and PS of both sides.

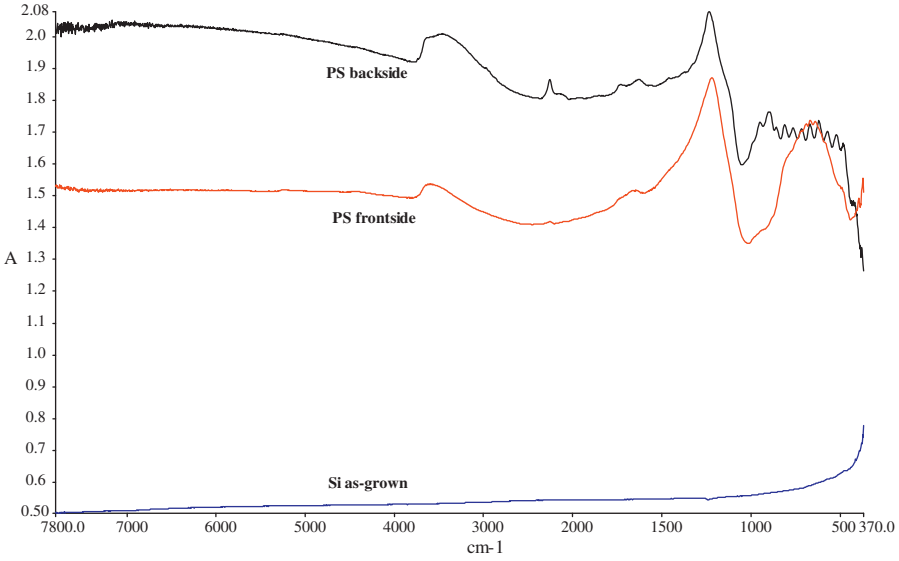

Fig. 7. FTIR absorption spectra of Si (as grown) and PS of both sides.

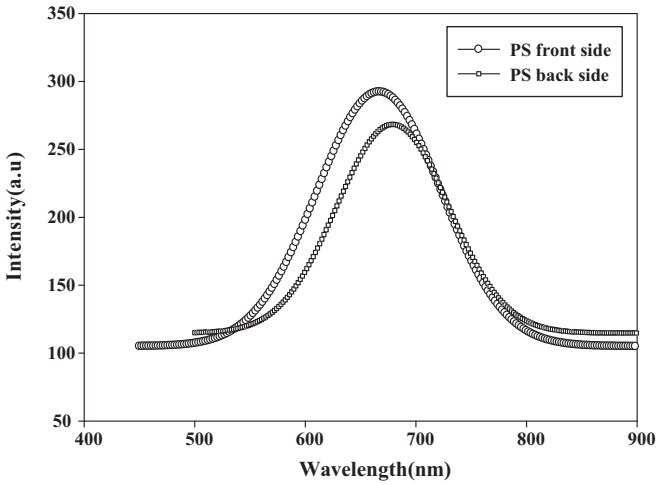

Fig. 8. PL spectra of PS on both sides of the c-Si wafer.

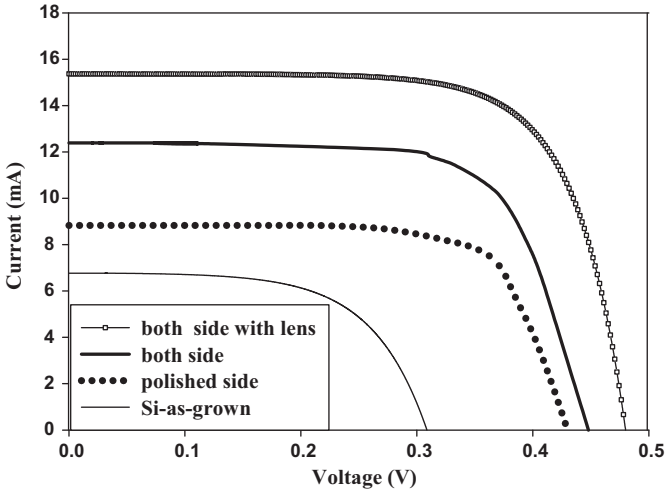

Fig. 9. Current–voltage (I–V) characteristics of Si (as grown) and Si of different sides.

The results are shown in Fig. 4 to demonstrate that PS formed on both sides has lower reflectivity value compared with the results of others [13–15] and these results have been confirmed by absorption spectrum as shown in Fig. 5. Figs. 6 and 7 show the FTIR spectra of the silicon as grown and PS as function of the reflectivity and absorptive, respectively. The results showed an agreement with the results demonstrated in Figs. 4 and 5. This means that our PS sample has a high absorption and low reflection spectrum as compared with the as grown sample and this may be attributed to the increase of porosity that leads to increase the PS density over the surface of the sample. Fig. 8 illustrates the PL spectrum of the PS formed on the unpolished side, revealing a peak at 681.3 nm (1.82 eV) with Full Width and Half Maximum (FWHM) of about 330 mV. For PS formed on the front polished side, the peak located at 666.9 nm (1.86 eV) with a FWHM of about 180 mV is obtained. PS formed on the front polished side revealed blue shift luminescence. This means particles are confined into the lower dimension. The energy gaps of PS are increased to 1.82 and 1.86, respectively. The broadening of the energy gap occurs with a decrease in the crystallite size.

The results in Figs. 4 and 8 are used to calculate the refractive index and optical dielectric constant of Si and PS using [18]:

$$n = \frac{1 + R^{1/2}}{1 - R^{1/2}} \tag{1}$$

where R is reflectivity. The results are given and compared with others in Table 1.

The refractive index n is an important physical parameter related to microscopic atomic interactions. Theoretically, the two different approaches in viewing this subject are the refractive index related to density, and the local polarizability of these entities [19].

On the other hand, the crystalline structure represented by a delocalized picture, n will be closely related to the energy band structure of the material, complicated quantum mechanical analysis requirements and the obtained results. Many attempts have been made to relate the refractive index and the energy gap E_g through simple relationships [20–25].

However, these relationships of n are independent of temperature and incident photon energy. Here, the various relationships between n and E_g will be reviewed. Ravindra et al. [25] suggested different relationships between the band gap and the high frequency refractive index and presented a linear form of n as a function of E_g:

$$n = \alpha + \beta E_g \tag{2}$$

where $\alpha = 4.048$ and $\beta = -0.62\ \mathrm{eV}^{-1}$.

To be inspired by simple physics of light refraction and dispersion, Herve and Vandamme [26] proposed an empirical relation as:

$$n = \sqrt{1 + \left(\frac{A}{E_g + B}\right)^2} \tag{3}$$

where $A = 13.6$ eV and $B = 3.4$ eV. Ghosh et al. [27] took a different approach to the problem by considering the band structural and quantum-dielectric formulations of Penn [28] and Van Vechten [29]. Introducing A as the contribution from the valence electrons and B as a constant additive to the lowest band gap E_g, the expression for the high-frequency refractive index is written as:

$$n^2 - 1 = \frac{A}{(E_g + B)^2} \tag{4}$$

where $A = 25E_g + 212$, $B = 0.21E_g + 4.25$ and $(E_g + B)$ refers to an appropriate average energy gap of the material. Thus, these three models of variation n with energy gap have been calculated. The calculated refractive indices of the end-point compounds are investigated in Table 1. The optical dielectric constant ε_∞ is calculated using $\varepsilon_\infty = n^2$ [30] and depends on the refractive index. In Table 1, the calculated values of ε_∞ using the three models are investigated. Increasing porosity percentage from 60% (front side) to 80% (back side) uses the weight measurements [31] leads to decreasing refractive index. As with Ghosh et al. [27], this is more appropriate for studying solar cell optical properties.

The series and sheet resistances, maximum voltage V_m, maximum current I_m, open-circuit voltage V_{oc}, and short-circuit current I_{sc} are the prominent parameters in calculating solar cell efficiency.

The increasing efficiency of solar cells fabricated with PS formed on both sides of the wafer compared with one side PS and bulk Si solar cells, respectively is shown in Fig. 9. This is attributed to increasing the open circuit voltage without losing the short circuit current of the solar cells, as shown in Table 2. The porous surface texturing properties could enhance and increase the conversion efficiency of Si solar cells. The results also showed that the efficiency resulting from this procedure is more promising compared with other solar cells fabricated under similar conditions [32].

Table 1
Calculated refractive indices for Si and PS using Ravindra et al. [25], Herve and Vandamme [26], and Ghosh et al. [27] models compared with others corresponding to optical dielectric constant.

Samples	n	ε_∞
Si as-grown	3.35[a] 2.91[b] 2.89[c] 3.46[d] 3.46[e]	11.22[a] 8.46[b] 8.35[c] 11.97[e]
PS formed on the unpolished side	3.17[a] 2.79[b] 2.77[c] 1.8[e]	10.04[a] 7.78[b] 7.67[c] 3.24[e]
PS formed on the front polished side	2.94[a] 2.68[b] 2.66[c] 2.38[e]	8.64[a] 7.18[b] 7.07[c] 5.66[e]

[a] Ref. [25].
[b] Ref. [26].
[c] Ref. [27].
[d] Ref. [18] expt.
[e] Using Eq. (1).

Table 2
Investigated series resistance R_s, sheet resistance R_{sh}, maximum voltage V_m, maximum current I_m, open-circuit voltage V_{oc}, short-circuit current I_{sc}, *FF*, and efficiency (η) of Si and PS.

Samples	R_s (Ω)	R_{sh} (kΩ)	V_m (V)	I_m (mA)	V_{oc} (V)	I_{sc} (mA)	*FF* (%)	Efficiency (η) (%)
Si as-grown	70.4	2.98	0.26	6.71	0.31	6.72	83	4.34
PS formed on the unpolished side	7.14	149.8	0.41	7.24	0.43	8.83	78	7.38
PS formed on both sides	7.9	4.86	0.44	11.65	0.49	12.37	84	12.75
PS both sides with lens	2.81	18.77	0.41	15.12	0.45	15.5	88	15.4

4. Conclusion

PS formed on the unpolished backside of the c-Si wafer showed an increase in surface roughness compared with one formed on the polished front side. The high degree of roughness along with the presence of the nanocrystal layer implies that the surface used as an ARC, which can reduce the reflection of light and increase light trapping on a wide wavelength range. This parameter is important in enhancing the photo conversion process for solar cell devices. PS formed on both sides has low reflectivity value. Fabricated Solar cells show that the conversion efficiency is 15.4% compared with the unetched sample and other results [13,15]. The results of the refractive index and optical dielectric constant of Si and PS are investigated. A good agreement with experimental data is observed.

Acknowledgments

Support from research university (RU) grant and Universiti Sains Malaysia is gratefully acknowledged. Also, Y.A. would like to acknowledge MOSTI, Malaysia of the BGM Program. In addition, thanks are due to TWAS-Italy, for full support of his visit to JUST-Jordan under TWAS-UNESCO Associateship.

References

[1] V.M. Aroutiounia, K.S.h. Martirosyana, S. Hovhannisyana, G. Soukiassianb, Use of porous silicon for double- and triple-layer antireflection coatings in silicon photovoltaic converters, J. Contemp. Phys. 43 (2008) 72.
[2] V.Y. Yerokhov, I.I. Melnyk, Porous silicon in solar cell structures: a review of achievements and modern directions of further use, Renew. Sustainable Energy Rev. 3 (1999) 291.
[3] L. Schirone, G. Sotgiu, M. Montecchi, A. Parisini, Porous silicon in high efficiency large area solar cells, in: Proc. 14th European PV Solar Energy Conf., 1997, p. 1479.
[4] P. Menna, G.D. Francia, V.L. Ferrara, Porous silicon in solar cells: a review and a description of its application as an AR coating, Solar Energy Mater. Solar Cells 37 (1997) 13.
[5] L. Schirone, G. Sotgiu, M. Montecchi, G. Righini, R. Zanoni, Stain etched porous silicon technology for large area solar cells, in: Proc. 2nd World Conf. PV Solar Energy Conversion, 1998, p. p276.
[6] R.B. Cláudia, R.B. Maurício, F.B. Antonio, G.F. Neidenêi, Morphological and optical characteristics of porous silicon produced by anodization in HF-ethanol solutions, J. Braz. Chem. Soc. 19 (2008) 76.
[7] P. Panek, M. Lipinski, H. Czternastek, Porous silicon layer as antireflection coating in solar cells, Opto-Electron. Rev. 8 (2000) 75.
[8] D.-H. Oha, T.W. Kim, W.J. Chob, KKD, Effects of a H_2SO_4 treatment on the optical. properties in porous Si layers and electrical properties of diode devices fabricated with a H_2SO_4 treated porous Si layer, J. Ceram. Process. Res. 9 (2008) 57.
[9] G. Barillaro, A. Nannini, F. Pieri, Porosity and dimension constraints of macropore arrays in n-doped silicon, J. Electrochem. Soc. C 180 (2002) 149.
[10] J. Guobin, S. Winfried, A. Tzanimir, K. Martin, Infrared light emission from porous silicon, J. Mater. Sci. Mater. Electron. 19 (2008) S9.
[11] F. Yan, X. Bao, T. Gao, Photovoltage spectra of silicon/porous silicon heterojunction, Solid State Commun. 91 (1994) 341.
[12] M. Yamaguchi, Super-high efficiency III–V tandem and multijunction cells, in: M.D. Archer, R. Hill (Eds.), Clean Electricity from Photovoltaics, Super-High Efficiency III–V Tandem and Multijunction Cells, Imperial College Press, London, 2001, p. 347.
[13] M. Ben Rabha, B. Bessaïs, Enhancement of photovoltaic properties of multicrystalline silicon solar cells by combination of buried metallic contacts and thin porous silicon, Solar Energy 84 (2010) 486.
[14] S. Yae, T. Kobayashi, T. Kawagishi, N. Fukumuro, H. Matsuda, Antireflective porous layer formation on multicrystalline silicon by metal particle enhanced HF etching, Solar Energy 80 (2006) 701.
[15] R. Brendel, Thin-film crystalline silicon mini-modules using porous Si for layer transfer, Solar Energy 77 (2004) 969.
[16] G. Lerondel, R. Romestain, in: L. Canham (Ed.), Reflection and Light Scattering in Porous Silicon, Properties of porous silicon, INSPEC, UK, 1997, p. 241.
[17] A. Ramizy, Z. Hassan, K. Omar, Porous silicon nanowires fabricated by electrochemical and laser-induced etching, J. Mater. Sci. Elect., (First available online), doi:10.1016/j.snb.2011.01.034.
[18] M.A. Mahdi, S.J. Kasem, J.J. Hassen, A.A. Swadi, S.K.J. Al-Ani, Structural and optical properties of chemical deposition CdS thin films, Int. J. Nanoelectron. Mater. 2 (2009) 163.
[19] N.M. Balzaretti, J.A.H. da Jornada, Pressure dependence of the refractive index of diamond, cubic carbide and cubic boron nitride, Solid State Commun. 99 (1996) 943.
[20] T.S. Moss, A relationship between the refractive index and the infra-red threshold of sensitivity for photoconductors, Proc. Phys. Soc. B 63 (1950) 167.
[21] V.P. Gupta, N.M. Ravindra, Comments on the Moss formula, Phys. Stat. Sol. B 100 (1980) 715.
[22] Y. Al-Douri, Electronic and optical properties of $Zn_xCd_{1-x}Se$, Mater. Chem. Phys. 82 (2003) 49.
[23] Y. Al-Douri, Y.P. Feng, A.C.H. Huan, Optical investigations using ultra-soft pseudopotential calculations of $Si_{0.5}Ge_{0.5}$alloy, Solid State Commun. 148 (2008) 521.
[24] P. Hervé, L.K.J. Vandamme, General relation between refractive index and energy gap in semiconductors, Infrared Phys. Technol. 35 (1994) 609.
[25] N.M. Ravindra, S. Auluck, V.K. Srivastava, On the Penn gap in semiconductors, Phys. Stat. Sol. (b) 93 (1979) K155.
[26] P.J.L. Herve, L.K.J. Vandamme, Empirical temperature dependence of the refractive index of semiconductors, J. Appl. Phys. 77 (1995) 5476.
[27] D.K. Ghosh, L.K. Samanta, G.C. Bhar, A simple model for evaluation of refractive indices of some binary and ternary mixes crystals, Infrared Phys. 24 (1984) 34.
[28] D.R. Penn, Wave-number-dependent dielectric function of semiconductors, Phys. Rev. 128 (1962) 2093.
[29] J.A. Van Vechten, Quantum dielectric theory of electronegativity in covalent systems I. Electronic dielectric constant, Phys. Rev. 182 (1969) 891.
[30] G.A. Samara, Temperature and pressure dependences of the dielectric constants of semiconductors, Phys. Rev. B 27 (1983) 3494.
[31] A. Halimaoui, in: L. Canham (Ed.), Porous Silicon Formation by Anodization Properties of Porous Silicon, INSPEC, UK, 1997, p. 18.
[32] J.A. Wisam, A. Ramizy, K. Ibrahim, Z. Hassan, K. Omar, The performance of silicon solar cell with different texturing processes, J. Optoelectron. Adv. Mater. 11 (2009) 1632.